Cytoplasmic Dynein Regulation by Subunit Heterogeneity and Its Role in Apical Transport

Andrew W. Tai,* Jen-Zen Chuang,‡ and Ching-Hwa Sung*‡

*Department of Cell Biology and Anatomy, and ‡Department of Ophthalmology, The Margaret M. Dyson Vision Research Institute, Weill Medical College of Cornell University, New York, New York 10021

Abstract. Despite the existence of multiple subunit isoforms for the microtubule motor cytoplasmic dynein, it has not yet been directly shown that dynein complexes with different compositions exhibit different properties. The 14-kD dynein light chain Tctex-1, but not its homologue RP3, binds directly to rhodopsin's cytoplasmic COOH-terminal tail, which encodes an apical targeting determinant in polarized epithelial Madin-Darby canine kidney (MDCK) cells. We demonstrate that Tctex-1 and RP3 compete for binding to dynein intermediate chain and that overexpressed RP3 displaces endogenous Tctex-1 from dynein complexes in MDCK cells. Furthermore, replacement of Tctex-1 by RP3 selectively disrupts the translocation of rhodopsin to the MDCK apical surface. These results directly show that cytoplasmic dynein function can be regulated by its subunit composition and that cytoplasmic dynein is essential for at least one mode of apical transport in polarized epithelia.

Key words: cytoplasmic dynein light chain • Tctex-1 • RP3 • apical transport • rhodopsin

Introduction

Cytoplasmic dynein, a multisubunit minus-end microtubule motor, appears to be able to recognize its cargoes in a spatially and temporally regulated manner, but we do not understand the basis of this regulation. A potential mechanism for generating dynein cargo binding selectivity is subunit heterogeneity, as several dynein subunits have been implicated as adapters between the dynein complex and specific cargo molecules (Steffen et al., 1997; Purohit et al., 1999; Puthalakath et al., 1999; Tai et al., 1999). There are as many as three or four known cytoplasmic dynein heavy chains (HCs),[1] perhaps each with a preferential tissue and subcellular localization (Vaisberg et al., 1996; Criswell and Asai, 1998). At least five distinct intermediate chain (IC) polypeptides are expressed in neurons (Pfister et al., 1996). Finally, two closely related 14-kD dynein light chains (LCs), named Tctex-1 and RP3, have recently been identified (King et al., 1996, 1998). Although there is much indirect evidence that dynein complexes with differing subunit compositions have different functions, a direct demonstration has not yet been performed.

The functions of polarized cells, including epithelial cells and neurons, are dependent on the generation and maintenance of plasma membrane asymmetry. Although the requirement for microtubule motors in fast axonal transport is well-established (Schnapp and Reese, 1989; Martin et al., 1999), the role of such motors in post-Golgi transport in polarized epithelial cells is not fully understood. The microtubules in polarized epithelial cells, such as Madin-Darby canine kidney (MDCK) cells, are longitudinally arrayed, with their minus and plus ends located at the apical and basal membranes, respectively (Bacallao et al., 1989). This arrangement poses the interesting possibility that a subset of apical and basolateral carrier vesicles use dynein and kinesin, respectively, to move from the TGN to their respective membrane destinations. This hypothesis has been further supported by the observation that intact microtubules are required for some apical protein targeting in polarized MDCK cells (Parczyk et al., 1989; Breitfeld et al., 1990). However, no in vivo evidence has yet been provided to demonstrate that dynein is required for the apical transport of a protein in polarized epithelial cells.

Rhodopsin, a phototransducing G protein–coupled receptor, is polarized to the photoreceptor outer segment in vivo; mutations in the cytoplasmic COOH terminus of rhodopsin prevent its correct polarization in photoreceptors (Sung et al., 1994; Li et al., 1996). Recently, we have shown that this region of rhodopsin functionally interacts with the dynein complex via the 14-kD dynein LC Tctex-1 (Tai et al., 1999). Interestingly, the cytoplasmic COOH ter-

A.W. Tai and J.-Z. Chuang contributed equally to this work.

Address correspondence to Ching-Hwa Sung, Department of Ophthalmology, The Margaret M. Dyson Vision Research Institute, Weill Medical College of Cornell University, 1300 York Ave., New York, NY 10021. Tel.: (212) 746-2291. Fax: (212) 746-6670. E-mail: chsung@mail.med.cornell.edu

[1]*Abbreviations used in this paper:* CMV, cytomegalovirus; GFP, green fluorescent protein; GST, glutathione *S*-transferase; HA, hemagglutinin; HC, heavy chain; IC, intermediate chain; LC, light chain; LDL, low density lipoprotein; LIC, light intermediate chain.

minus of rhodopsin is also required for the apical targeting of rhodopsin in polarized MDCK cells (Chuang and Sung, 1998). Thus, it is likely that the polarized distribution of rhodopsin in MDCK cells, as in rod photoreceptors, is mediated by the direct interaction of rhodopsin's cytoplasmic apical targeting signal with cytoplasmic dynein.

Our previous observation that Tctex-1, but not its homologue RP3, interacts with rhodopsin's COOH terminus (Tai et al., 1999), prompted us to hypothesize that RP3-containing dynein complexes would not be able to interact with rhodopsin. In this report, we show that ectopic expression of RP3 in MDCK cells displaces endogenous Tctex-1 from the cytoplasmic dynein complex. Such displacement results in the selective missorting of rhodopsin, as well as a subset of endogenous apical proteins in MDCK cells. Our data represent functional evidence that Tctex-1–mediated dynein function is essential for the apical targeting of some membrane proteins in polarized epithelia. Taken together, our results demonstrate directly that dynein's cargo specificity, and hence function, can be regulated by its subunit composition.

Materials and Methods

Reagents and Antibodies

All reagents were obtained from Sigma-Aldrich unless otherwise specified. The following antibodies were used: dynein IC mAb (clone 74.1; Chemicon), anti-FLAG mAb (clone M2; Eastman Kodak Co.), $p150^{Glued}$ mAb (clone 1; Transduction Labs), rhodopsin mAb (clone B6-30; Dr. P. Hargrave [University of Florida, Gainesville, FL]; Adamus et al., 1988), GOS-28 mAb (Dr. W. Hong [Institute of Molecular and Cell Biology, Singapore]; Subramaniam et al., 1996), gp135 mAb (Dr. G.K. Ojakian [State University of New York at Brooklyn, Brooklyn, NY]; Ojakian and Schwimmer, 1988), pan-cadherin mAb (clone CH-19; Sigma-Aldrich), CD7 mAb (clone 3A1, American Type Culture Collection), low density lipoprotein (LDL) receptor mAb (Calbiochem); Na,K-ATPase mAb (Dr. M. Caplan [Yale University School of Medicine, New Haven, CT]), attenuated adenovirus particles (Dr. N.L. Weigel [Baylor College of Medicine, Houston, TX]; Allgood et al., 1997), influenza virus, influenza virus hemagglutinin (HA) rabbit antiserum, and LDL receptor adenovirus (Dr. E. Rodriguez-Boulan [Weill Medical College at Cornell University, New York, NY]). Alexa 488–conjugated goat anti–rabbit and Alexa 594–conjugated goat anti–mouse secondary antibodies were obtained from Molecular Probes. Rabbit antiserum against rhodopsin was generated by using a maltose binding protein–rhodopsin COOH terminus fusion protein as an immunogen. Affinity-purified Tctex-1 and RP3 antibodies were prepared using the procedures described in Tai et al. (1998). These two antibodies are specific for their corresponding antigens and do not cross react with each other (Chuang, et al., 2001).

Plasmids and Adenoviral Vector Generation

The plasmids encoding glutathione *S*-transferase (GST)–Tctex-1 and GST-RP3 were described in Tai et al. (1998). Constructs for in vitro transcription/translation were prepared by inserting FLAG-tagged Tctex-1 and RP3 downstream of the T7 promoter in pBluescript II SK(−) (Stratagene). For eukaryotic expression of RP3, FLAG-tagged RP3 was subcloned into the mammalian expression vector pRK-5 (BD PharMingen) under the control of a cytomegalovirus (CMV) promoter. Green fluorescent protein (GFP) was expressed using the pEGFP-c1 vector (CLONTECH Laboratories, Inc.). For tetracycline-regulated FLAG-RP3, the EGFP coding sequence in the vector pBI-EGFP (CLONTECH Laboratories, Inc.) was replaced by the coding sequence for FLAG-RP3, thus placing the FLAG-RP3 sequence downstream of a minimal CMV promoter under the control of a tetracycline-responsive element. Details for all of the above subcloning strategies are available on request.

A recombinant adenoviral vector (Ad-CMV-Rho) encoding human rhodopsin under the control of the CMV promoter was generated and purified using techniques described in Graham and van der Eb (1973).

Blot Overlay Assay

0.5 μg of purified rat brain cytoplasmic dynein (purified as described in Tai et al. [1999]) was separated on SDS-PAGE and transferred to nitrocellulose. The membrane was blocked in TBS plus 2% BSA overnight at 4°C, then incubated in TBS-T (TBS/0.05% Tween-20) with 2% BSA for 1 h at room temperature. [^{35}S]-labeled FLAG-tagged Tctex-1 or RP3 was synthesized in vitro using the TnT-coupled transcription/translation system (Promega). After synthesis, unincorporated radiolabel was removed by Sephadex G-25 spin columns (Amersham Pharmacia Biotech). [^{35}S]FLAG–Tctex-1 or RP3 was added to the membrane at $1x10^6$ cpm/mL in TBS-T/0.5% BSA for 4 h at 4°C. After multiple washes in TBS-T/0.5% BSA at room temperature, the blot was dried and autoradiographed to detect bound Tctex-1 or RP3.

In Vitro Competition Assay

Purified GST, GST-Tctex-1, GST-RP3, or mock control was preincubated with TnT reaction mixture at a final concentration of 0.25 mg/mL for 45 min at room temperature before the addition of [^{35}S]methionine and DNA template encoding either FLAG–Tctex-1 or FLAG-RP3. After completion of the reactions, IC was immunoprecipitated using anti-IC mAb 74.1. The immunoprecipitates were then separated by SDS-PAGE and autoradiographed to detect the presence of coimmunoprecipitated [^{35}S]FLAG–Tctex-1 or RP3. Immunoprecipitation was also performed using anti-FLAG mAb to demonstrate that the amount of synthesized [^{35}S]FLAG–Tctex-1 or FLAG-RP3 used for IC immunoprecipitation was roughly equal for all competitors.

Cell Culture and Transfection/Infection

MDCK cells and MDCK-derived cell lines (Chuang and Sung, 1998 and see below) were grown in Dulbecco's modified Eagle medium (Life Technologies) supplemented with 10% fetal bovine serum, 100 U/mL of penicillin, 100 μg/mL of streptomycin, and additional antibiotics as described below. All cell cultures were maintained in 5% CO_2 at 37°C. Transient and stable transfections were performed using Lipofectamine PLUS (Life Technologies). For transient transfections, cells were transfected at ~50% confluence on 10-cm dishes and then plated at high density (~4×10^5 cells/cm^2) onto 12-mm Transwell filters (Corning-Costar). Filters were cultured for 5 d to obtain polarized monolayers for immunocytochemical assays.

The MDCK/T23 cell line (gift of Dr. K. Mostov [University of California at San Francisco, San Francisco, CA]; Barth et al., 1997) was used for inducible expression of FLAG-RP3. The T23 cell line stably expresses the tetracycline-controlled transactivator. As a result, the expression of genes under the control of a tetracycline-responsive element can be activated in MDCK/T23 cells by withdrawal of doxycycline from the medium. Stable T23 cell lines inducibly expressing FLAG-RP3 (T23/FLAG-RP3) were generated by transfection with a FLAG-RP3 construct under the control of a tetracycline response element (see above). Stable lines were obtained by selection in 200 μg/mL hygromycin and 100 ng/mL doxycycline to maintain FLAG-RP3 repression. For polarity assays, cells were plated at high density onto 24-mm Transwell filters and allowed to form polarized monolayers.

For rhodopsin and LDL receptor adenoviral infections, MDCK and T23/FLAG-RP3 polarized monolayers were infected at a titer of ~5×10^8 particles/cm^2 (Henkel et al., 2000). Cells were used 24 h after infection for immunocytochemistry or polarity assays. The efficiency of adenoviral infection was not affected by FLAG-RP3 expression. Neither induction of FLAG-RP3 expression nor adenovirus infection affected the transepithelial resistance of the polarized monolayer. CD7-Rho39 expression plasmid was introduced into polarized T23/FLAG-RP3 monolayer using the adenovirus particle-mediated transfection procedures described in (Allgood et al., 1997). In brief, attenuated adenoviral particles (1,000 particles/cell; Allgood et al., 1997) was mixed with CD7-Rho39 expression plasmid in poly-L-lysine (1.3 μg/μg DNA)–containing HBS buffer (150mM NaCl, 20 mM Hepes, pH 7.3). This virus–DNA mixture was added to MDCK monolayers for 2 h and returned to regular medium for 24 h before the assay.

For influenza virus infections, T23/FLAG-RP3–polarized monolayers were infected with the WSN strain (Rodriguez-Boulan, 1983). Cells were used 6–8 h after infection for immunocytochemistry.

Immunocytochemistry

Cells grown on coverslips or on Transwell filters were fixed in 4% paraformaldehyde in PBS plus 0.2 mM $CaCl_2$ and 2 mM $MgCl_2$ for 20 min at room temperature. The immunostaining procedures were performed as de-

scribed for coverslips (Tai et al., 1998) and for Transwell filters (Chuang and Sung, 1998).

Velocity Density Gradient Sedimentation

Three 10-cm dishes of T23/FLAG-RP3 cell lines were grown in the presence (uninduced condition) or absence (induced condition) of doxycycline (100 ng/mL) for 3 d and then harvested by scraping into PBS. After pelleting, the cells were resuspended in 80 mM PIPES, pH 6.8, 1 mM EGTA, 1 mM $MgSO_4$, 0.5 mM DTT, and protease inhibitors (1 mM PMSF, 2 μg/mL aprotinin, 2 μg/mL leupeptin, and 0.7 μg/mL pepstatin). The cells were homogenized by three passes through a ball-bearing homogenizer and then centrifuged at 100,000 *g* (TLA 100.3 rotor; Beckman Coulter) for 20 min at 4°C. The high-speed supernatants were then separated by velocity sedimentation on 5–20% linear sucrose gradients (Paschal et al., 1991). 12 fractions of 1 mL each were collected from the bottom of the tube, and 20-μL samples from each fraction were used for SDS-PAGE and immunoblotting. The gradients were calibrated with thyroglobulin (19S) and catalase (11.3S) standards.

Domain-selective Surface Biotinylation/Membrane Targeting Assay

For the microtubule depolymerization experiments, a rhodopsin-expressing MDCK stable line grown on Transwell filters (Chuang and Sung, 1998) was treated with 33 μM nocodazole (33 mM stock in DMSO) or 0.1% DMSO at 4°C for 30 min followed by incubation at 37°C for 3.5 h to depolymerize microtubules. Microtubule depolymerization was confirmed by α-tubulin immunostaining of duplicate filters. Nocodazole treatment did not affect MDCK transepithelial resistance (data not shown; Ojakian and Schwimmer, 1988; Parczyk et al., 1989). The cells underwent pulse–chase labeling with [^{35}S]cysteine/methionine (New England Nuclear) in the presence of nocodazole or DMSO. At each chase timepoint, cells were chilled on ice and processed for domain-selective surface biotinylation (Chuang and Sung, 1998). In brief, glycosylated surface proteins were selectively biotinylated from either the apical or basolateral side using biotin-LC-hydrazide (Pierce Chemical Co.). Cells on excised filters were lysed in 50 mM Tris, pH 7.4, 150 mM NaCl, 2 mM EDTA, 1% Triton X-100, and protease inhibitors at 4°C for 30 min. After centrifugation of the lysate at 14,000 *g* for 15 min, biotinylated rhodopsin was isolated by sequential immunoprecipitation with rhodopsin mAb B6-30 followed by binding to streptavidin-agarose (Pierce Chemical Co.). The biotinylated rhodopsin was then separated by SDS-PAGE, transferred to nitrocellulose, and the amount of radiolabeled rhodopsin was quantitated by phosphorimaging using a Storm scanner (Molecular Dynamics).

To measure the surface distribution of rhodopsin in FLAG-RP3–expressing cells, T23/FLAG-RP3 cells were plated at low density in the presence or absence of doxycycline for 3 d before plating at high density (1.5×10^6 per well) onto 24-mm Transwell filters. After 5 d, polarized monolayers were infected with Ad-CMV-Rho for 24 h followed by biotin-LC-hydrazide surface labeling from either side. Rhodopsin was immunoprecipitated from the cell lysates with B6-30 mAb. Immunoprecipitated rhodopsin was then separated by SDS-PAGE and transferred to a nitrocellulose membrane. Finally, biotinylated rhodopsin was visualized using horseradish peroxidase–conjugated streptavidin (Kirkegaard and Perry Laboratories) and ECL-Plus (Amersham Pharmacia Biotech) followed by quantitation of chemifluorescence using a Storm scanner. The linearity of this detection system for the amounts of rhodopsin expressed was confirmed using biotinylated protein standards (data not shown).

For measurement of rhodopsin targeting in FLAG-RP3 expressing cells, T23/FLAG-RP3 cells were plated and infected with Ad-CMV-Rho as described above. The cells were then pulse labeled with [^{35}S]cysteine/methionine for 30 min. At each chase timepoint (0, 1, and 2 h), cells were chilled on ice and processed for domain-selective surface biotinylation as described above. After centrifugation of the lysate at 14,000 *g* for 15 min, biotinylated rhodopsin was isolated by sequential immunoprecipitation with rhodopsin mAb B6-30 followed by binding to streptavidin-agarose. 10% of the B6-30 immunoprecipitate was retained to correct for filter-to-filter variability in [^{35}S]incorporation into rhodopsin. All samples underwent cleavage of their N-glycans by digestion with N-glycanase (Glyko) to simplify quantitation (Sung et al., 1991). The biotinylated rhodopsin was then separated by SDS-PAGE, transferred to nitrocellulose, and the amount of radiolabeled rhodopsin was quantitated by phosphorimaging.

For the study of endogenous apical proteins in MDCK cells, T23/FLAG-RP3 cells were induced/uninduced and polarized on Transwell filters as described in the preceding paragraph. After 5 d, polarized monolayers were metabolically labeled with [^{35}S]cysteine/methionine from the basolateral side for 4 h, chased for 1 h, and then selectively biotinylated from the apical side using sulfo-NHS-LC-biotin (Pierce Chemical Co.), which reacts with primary amines. Doxycycline was included during the labeling and chase periods for uninduced filters. After lysis, biotinylated apical proteins were recovered by streptavidin-agarose precipitation and the total recovery was quantitated by liquid scintillation counting. Equal amounts of radiolabeled biotinylated protein recovered from the apical surface were separated using two-dimensional electrophoresis (O'Farrell, 1975) by Kendrick Laboratories. Isoelectric focusing was carried out using 2.0% pH 3.5–10 ampholines (Amersham Pharmacia Biotech) in 2.0-mm i.d. glass tubes. After equilibration for 10 min in 10% glycerol, 50 mM DTT, 2.3% SDS, and 62.5 mM Tris-HCl, pH 6.8, the tube gel was sealed to the top of a stacking gel overlaying a 10% acrylamide slab gel. After SDS slab gel electrophoresis, the gels were treated with En^{3}Hance (New England Nuclear) for 1 h, rehydrated in water for 30 min, dried onto filter paper, and autoradiographed.

Results

Tctex-1 and RP3 Interact Directly with and Compete for Binding to Dynein IC In Vitro

The two 14-kD dynein LCs, Tctex-1 and RP3, are closely related, sharing 52% identity and 75% similarity (King et al., 1996; Tai et al., 1998). Their high degree of similarity to one another suggested that they could interact with the same cytoplasmic dynein subunit.

To identify the dynein subunit that interacted with the 14-kD LCs, we used a blot overlay interaction assay. Purified rat brain cytoplasmic dynein was separated by SDS-PAGE and transferred to nitrocellulose. The membrane was probed with in vitro–translated, [^{35}S]-labeled, FLAG-tagged Tctex-1 or RP3. As shown in Fig. 1 A, both Tctex-1 (middle) and RP3 (right) interacted with a protein migrating with an apparent molecular weight consistent with that of dynein IC. Immunoblotting confirmed that the blot-overlay signal comigrated exactly with the band recognized by an mAb against IC (data not shown). No other interacting proteins were detected. It is likely that both LCs interact directly with IC, as no other interacting dynein–dynactin subunits were detected. Furthermore, KI disruption of the cytoplasmic dynein complex yields a IC–LC subcomplex (King et al., 1998), and structural analysis indicates that Tctex-1 binds directly to IC (Mok et al., 2001).

We then tested whether Tctex-1 and RP3 could compete with one another for binding to dynein. To this end, we noted that in vitro–synthesized FLAG–Tctex-1 and RP3 could be immunoprecipitated with an mAb against the endogenous IC present in the in vitro translation mixture (Fig. 1 B, lanes 7 and 11). The interaction between [^{35}S]FLAG–Tctex-1 and IC could be blocked by the prior addition of excess unlabeled purified GST–Tctex-1 but not by GST alone (Fig. 1 B, lanes 8 and 9). Moreover, the binding of [^{35}S]FLAG–Tctex-1 to IC could also be blocked by excess GST-RP3 (Fig. 1 B, lane 10). Likewise, the binding of [^{35}S]FLAG-RP3 to IC could be blocked by GST fusions of either Tctex-1 or RP3, but not by GST alone (Fig. 1 B, lanes 12–14). Note that the addition of the GST fusion proteins had no effect on the amounts of Tctex-1 or RP3 synthesized (Fig. 1 B, lanes 1–6). These results are consistent with a model in which Tctex-1 and RP3 share identical or overlapping binding sites on IC and thus compete with one another for binding to the dynein complex.

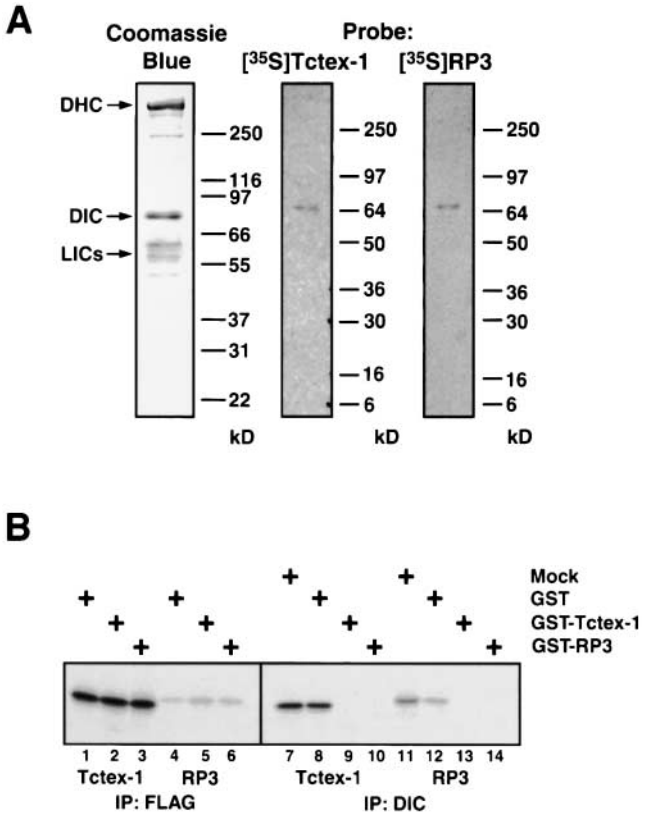

Figure 1. Competition between Tctex-1 and RP3 for binding to dynein IC. (A) Tctex-1 and RP3 were tested for their ability to bind to cytoplasmic dynein subunits in a blot overlay assay. Purified rat brain cytoplasmic dynein was separated by SDS-PAGE. The Coomassie blue–stained lane reveals the dynein subunits (left panel). Duplicate lanes were transferred to nitrocellulose and probed with [^{35}S]-labeled, in vitro–translated, FLAG-tagged Tctex-1 (middle) or RP3 (right). After washing, bound [^{35}S]FLAG–Tctex-1 or FLAG-RP3 was visualized by autoradiography. (B) Competition between Tctex-1 and RP3 for binding to IC. In vitro–translated, [^{35}S]-labeled FLAG–Tctex-1 and FLAG-RP3 were immunoprecipitated with anti-FLAG antibody to show that the total amount of translated [^{35}S]FLAG–Tctex-1 or RP3 was unaffected by the addition of unlabeled competitors (lanes 1–6). FLAG–Tctex-1 and FLAG-RP3 were also immunoprecipitated by an mAb against the endogenous IC present in the translation mixture (lanes 7 and 11). Addition of excess unlabeled GST–Tctex-1 blocked the association of [^{35}S]FLAG–Tctex-1 (lane 9) as well as [^{35}S]FLAG-RP3 (lane 13) with IC. Similarly, excess unlabeled GST-RP3 blocked the association of [^{35}S]FLAG–Tctex-1 (lane 10) and [^{35}S]FLAG-RP3 (lane 14) with IC. GST alone had no effect on the binding of either LC to IC (lanes 8 and 12).

Elevated Expression of RP3 Leads to Loss of Tctex-1 Immunofluorescence in Cell Culture

We then examined the effect of ectopically overexpressed RP3 on endogenous Tctex-1's intracellular expression and/or distribution in vivo. We found, to some surprise, that transient transfection of MDCK cells with FLAG-RP3 dramatically decreased endogenous Tctex-1 immunofluorescence to nearly undetectable levels (Fig. 2 A). The Tctex-1 suppression resulting from RP3 overexpression was confirmed by both immunostaining and immunoblotting in stable MDCK cell lines (see Figs. 4 A and 6 D). On the other hand, transient overexpression of control GFP had no effect on Tctex-1 levels (Fig. 2 B). Although the molecular mechanism underlying the reduction of Tctex-1 expression is not yet clear, it is likely to be related to the ability of RP3 to displace Tctex-1 from the dynein complex (see below).

Ectopically Expressed RP3 Is Structurally Incorporated into Dynein

To study the incorporation of ectopically expressed FLAG-RP3 into the dynein complex in vivo, we examined the distribution of FLAG-RP3 along with dynein IC (Fig. 3 A) and p150^{Glued}, a dynactin subunit (Fig. 3 C), in transiently transfected MDCK cells.

In interphase cells, FLAG-RP3 immunostaining was found primarily in a punctate distribution (Fig. 3, B and D). Like endogenous Tctex-1 (data not shown), transfected FLAG-RP3 colocalized extensively with IC, suggesting that FLAG-RP3 had become associated with endogenous cytoplasmic dynein complexes (Fig. 3, A and B). Similarly, we observed extensive colocalization of punctate FLAG-RP3 staining with the dynactin subunit p150^{Glued} (Fig. 3, C and D). The punctate structures labeled by each of these antibodies likely represent microtubule plus ends (Vaughan et al., 1999). Double labeling with α-tubulin showed that FLAG-RP3 had no detectable effect on microtubule organization in MDCK cells (not shown).

To further study the effects of RP3 overexpression using biochemical techniques, we generated MDCK/T23 stable lines inducibly expressing FLAG-RP3 (henceforth referred to as T23/FLAG-RP3 cells). In these cells, FLAG-RP3 expression could be induced by the removal of doxycycline from the medium, and we verified such induction in these cells by immunostaining (data not shown) and immunoblotting of cell lysates (Fig. 4 A, panel 4). RP3 induction was accompanied by a reduction of Tctex-1 protein to undetectable levels (Fig. 4 A, panel 3). Consistent with the immunofluorescence results in transiently transfected cells, the amount of IC or the dynactin subunit p150^{Glued} did not change upon RP3 induction (Fig. 4 A, panels 1 and 2).

To confirm biochemically that ectopically expressed RP3 displaces Tctex-1 from the dynein complex in vivo, cytosol from induced and uninduced T23/FLAG-RP3 cells was fractionated by velocity density gradient sedimentation. Aliquots from the gradient fractions were immunoblotted for IC, p150^{Glued}, FLAG-RP3, and Tctex-1. Both cytoplasmic dynein and dynactin typically sediment at 20S (Paschal et al., 1987; Schroer and Sheetz, 1991). We found no differences in the sedimentation behavior of cytoplasmic dynein or dynactin from induced or uninduced T23/FLAG-RP3 cells (Fig. 4 B). In uninduced cells, the majority of endogenous Tctex-1 cofractionated with dynein, whereas in induced cells, little or no Tctex-1 was detected (Fig. 4 B, panels 3 and 7). Instead, a portion of FLAG-RP3 cofractionated with IC, consistent with its incorporation into the cytoplasmic dynein complex (Fig. 4 B, panel 6).

Ectopically Expressed RP3 Does Not Disrupt General Dynein Activities

Cytoplasmic dynein is known to be involved in the centrosomal localization of the Golgi apparatus (Corthésy-

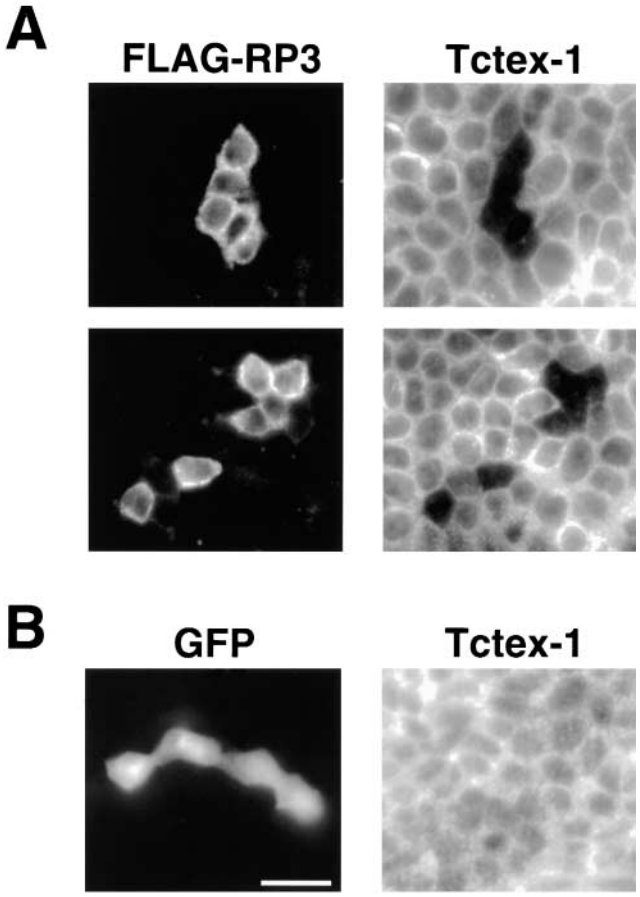

Figure 2. Loss of endogenous Tctex-1 protein by ectopic expression of RP3. MDCK cells were transiently transfected with expression vectors encoding FLAG-RP3 (A) or GFP (B) and then allowed to polarize on Transwell filters. After fixation, cells were immunolabeled with either anti-FLAG and Tctex-1 antibodies (A) or Tctex-1 antibody alone (B). Bar, 20 μm.

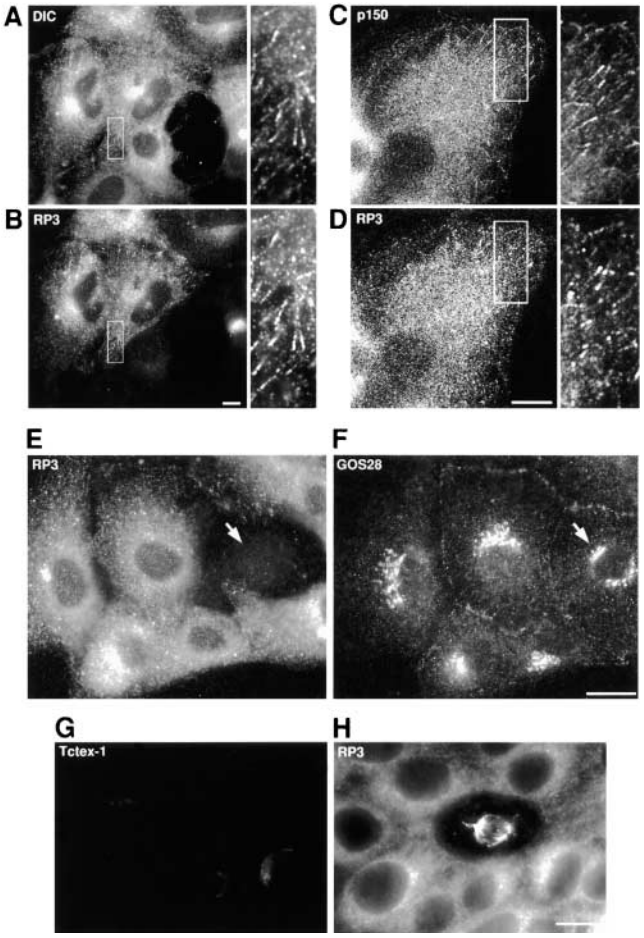

Figure 3. Ectopically expressed RP3 colocalizes with endogenous dynein–dynactin and does not alter Golgi complex organization or the mitotic spindle. (A–D) Subconfluent MDCK cells were transiently transfected with a FLAG-RP3 expression vector. Transfected cells were double-labeled with RP3 antibody (B and D) and mAbs against IC (A) and $p150^{Glued}$ (C). The boxed regions in the left panels in A–D are enlarged in the right panels. (E and F) Subconfluent MDCK cells transiently transfected with FLAG-RP3 were double-labeled with RP3 antibody (E) and an mAb against the Golgi v-SNARE GOS-28 (F). The arrow indicates a nontransfected cell. (G and H) An example of a mitotic FLAG-RP3–expressing cell is shown. Transfected MDCK cells were double-labeled with FLAG mAb (H) and Tctex-1 antibody (G). Bars: (B and D) 10 μm; (F) 20 μm; (H) 10 μm.

Theulaz et al., 1992). Disruption of general dynein function, such as microinjection of IC antibodies and overexpression of dynactin subunits, results in dispersal of the Golgi apparatus throughout the cytoplasm (Vaisberg et al., 1996; Burkhardt et al., 1997; Harada et al., 1998). However, staining for the Golgi v-SNARE GS28/GOS28 (Subramaniam et al., 1996) did not show any alteration in the morphology or distribution of the Golgi complex in RP3-transfected MDCK cells compared with neighboring nontransfected cells (Fig. 3, E and F). Furthermore, the distributions of transferrin receptor (recycling and early endosomes) and LAMP-1 (late endosomes and lysosomes) were not perturbed at the light microscopic level in RP3-expressing MDCK cells (data not shown).

In transfected mitotic cells, FLAG-RP3 was located on mitotic spindles (Fig. 3 H), which is consistent with the known mitotic spindle localization of cytoplasmic dynein (Steuer et al., 1990) and Tctex-1 in particular (Campbell et al., 1998; Tai et al., 1998). Despite the absence of endogenous Tctex-1 on mitotic spindles in FLAG-RP3–expressing cells (Fig. 3 G), no obviously aberrant mitotic spindles could be found among mitotic FLAG-RP3–expressing cells. Moreover, FLAG-RP3–expressing cells were not found to be blocked at any particular stage in mitosis (data not shown). These results suggest that RP3-containing cytoplasmic dynein is capable of carrying out general dynein-mediated cellular functions.

Microtubule Disruption Inhibits the Apical Delivery of Rhodopsin in MDCK Cells

To test whether Tctex-1/cytoplasmic dynein is involved in the apical transport of rhodopsin in polarized MDCK cells, we first examined whether apical rhodopsin expression in MDCK cells was dependent on microtubule integrity. MDCK cells stably expressing rhodopsin were allowed to form polarized monolayers on Transwell filters. Microtubules were depolymerized by nocodazole before and during metabolic pulse labeling with [^{35}S]cysteine/methionine. At various chase times, the distribution of la-

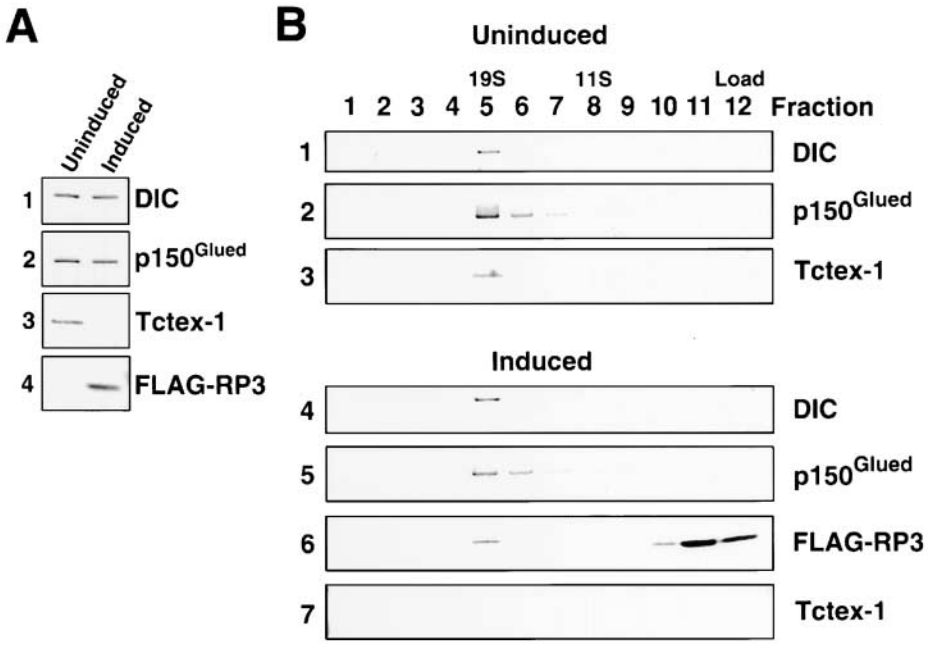

Figure 4. Replacement of cytoplasmic dynein–associated Tctex-1 by RP3 in MDCK cells. (A) Total cell lysates prepared from uninduced (left) and induced (right) T23/FLAG-RP3 cells were separated by SDS-PAGE and immunoblotted for IC (1), p150^{Glued} (2), Tctex-1 (3), and FLAG-RP3 (4). (B) High-speed supernatants prepared from homogenates of uninduced (1–3) and induced (4–7) T23/FLAG-RP3 cells were separated by velocity sedimentation on sucrose gradients. Aliquots from all fractions were separated on SDS-PAGE and immunoblotted for IC (1 and 4), p150^{Glued} (2 and 5), Tctex-1 (3 and 7), and FLAG-RP3 (6). Thyroglobulin (19 S) and catalase (11 S) were used as standards.

beled plasma membrane rhodopsin in nocodazole-treated versus mock-treated cells was assayed by a domain-selective surface biotinylation/membrane targeting assay.

Rhodopsin was highly polarized at the apical plasma membrane at 1 h chase in mock-treated cells, suggesting that rhodopsin is directly transported from the TGN to the apical surface (Fig. 5). In contrast, nocodazole treatment resulted in a significant reduction of rhodopsin polarity at all chase times studied. This finding suggests that the vectorial transport of newly synthesized rhodopsin to the apical surface in MDCK cells requires intact microtubules. On the other hand, cytochalasin D, which disrupts microfilaments, had no effect on rhodopsin apical polarity (data not shown).

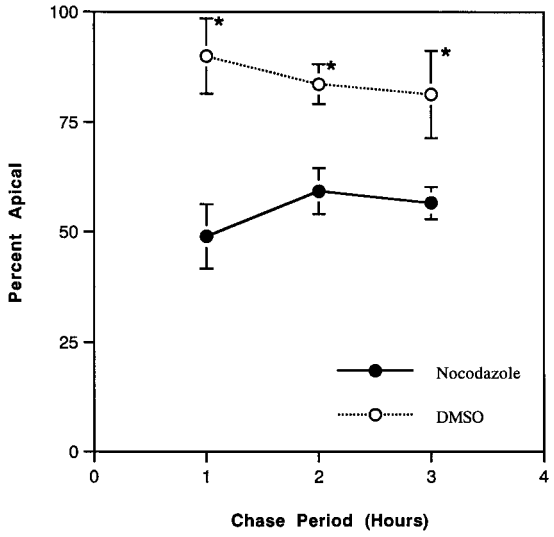

Figure 5. Requirement for intact microtubules in the apical delivery of rhodopsin in MDCK cells. Polarized MDCK cells stably expressing rhodopsin were treated with nocodazole (filled circles) or mock treated (open circles) and metabolically labeled with [^{35}S]cysteine/methionine. At the chase times shown, the fraction of total surface rhodopsin on the apical plasma membrane was assayed by domain-selective surface biotinylation. The means and standard deviations for three independent trials using duplicate filters are shown. Asterisk, $P < 0.02$ for nocodazole treatment relative to mock treatment by two-sided, two sample t test.

Downregulation of Tctex-1 Expression Leads to the Specific Missorting of Rhodopsin in MDCK Cells

The finding that intact microtubules are required for the polarized apical delivery of rhodopsin in MDCK cells is consistent with a role for cytoplasmic dynein in rhodopsin transport. We then proceeded to study rhodopsin trafficking in MDCK cells in which endogenous Tctex-1 had been suppressed by RP3 overexpression.

First, we examined rhodopsin polarity in MDCK cells transiently transfected with FLAG-RP3. In these experiments, transfected cells were allowed to become polarized on Transwell filters and were then infected with an adenoviral vector encoding rhodopsin. Using double immunofluorescent labeling, we observed that rhodopsin was distributed in a nonpolarized manner in RP3-transfected cells, whereas rhodopsin was apically expressed in untransfected cells expressing normal levels of endogenous Tctex-1 (Fig. 6 A). Overexpression of GFP did not affect rhodopsin polarity in MDCK cells (Fig. 6 B). Moreover, the randomization of rhodopsin plasma membrane targeting was unlikely to be due to nonspecific effects of dynein LC overexpression, because rhodopsin apical polarity was not affected by overexpression of FLAG-Tctex-1 (Fig. 6 C).

The prevention of rhodopsin's apical targeting was confirmed in stable MDCK T23/FLAG-RP3 cell lines, in which RP3 expression (or endogenous Tctex-1 suppression) was regulated by tetracycline withdrawal. In these experiments, rhodopsin was apically expressed in uninduced cells, whereas the loss of endogenous Tctex-1 caused by induction of FLAG-RP3 expression resulted in a nonpolar distribution of rhodopsin (Fig. 6 D).

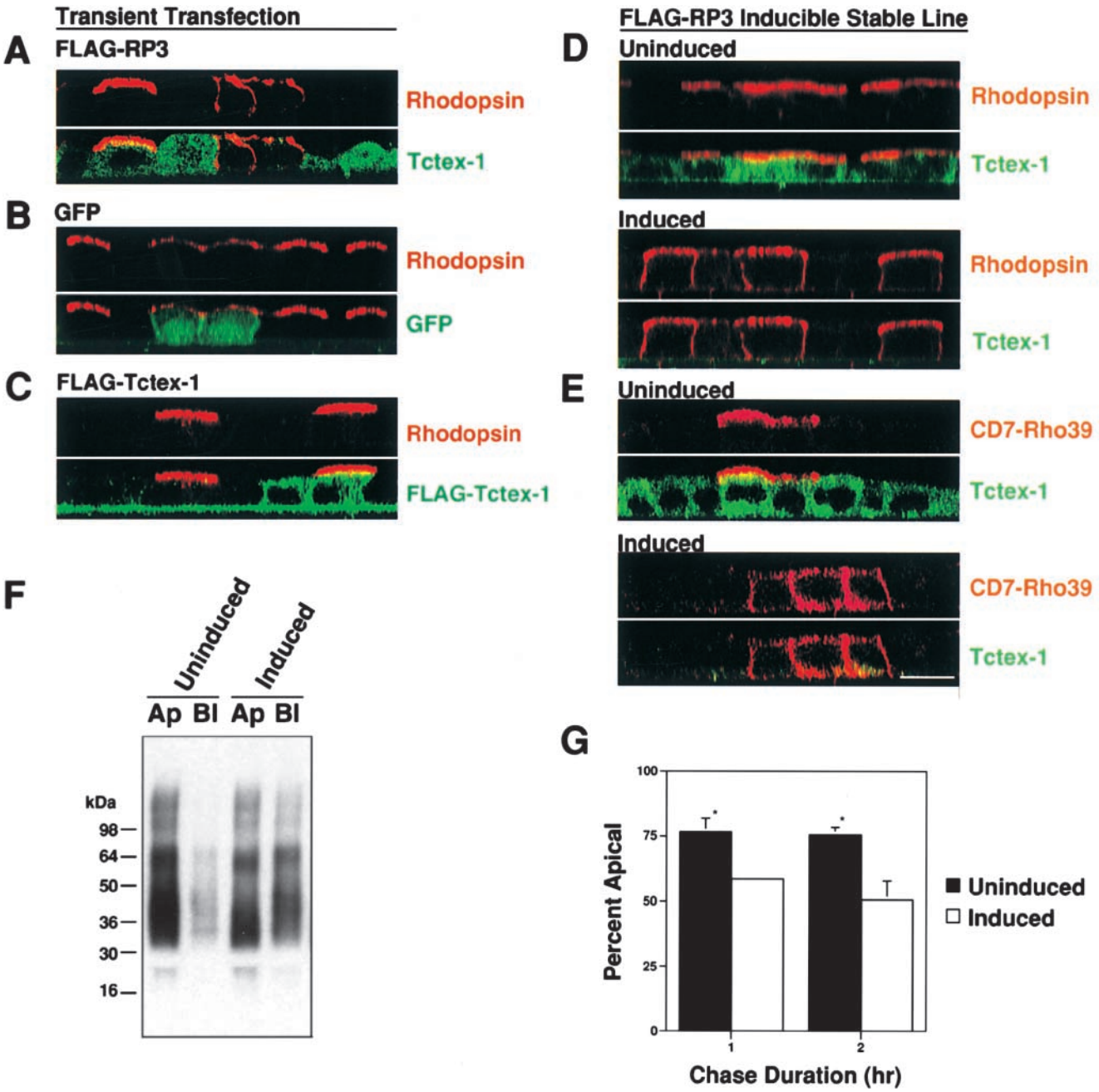

Figure 6. Specific inhibition of rhodopsin's apical polarity in MDCK cells by Tctex-1 downregulation. (A–C) MDCK cells were transiently transfected with FLAG-RP3 (A), GFP (B), or FLAG–Tctex-1 (C) and then allowed to form polarized monolayers. Monolayers were then infected with rhodopsin adenovirus for 24 h. Cells were double-labeled with Tctex-1 rabbit antibody (green) and rhodopsin mAb (red) in A. Cells were singly labeled with rhodopsin mAb (red; GFP is green) in B. In these experiments, FLAG-RP3–transfected cells are identifiable by their loss of endogenous Tctex-1 expression. In C, cells were doubled labeled with antirhodopsin rabbit antibody (red) and anti-FLAG mAb (green). Confocal sections in the x-z plane is shown, with the apical surface toward the top of the frame. (D) T23/FLAG-RP3 cells were left uninduced (top) or were induced to express FLAG-RP3 (bottom) before infection with rhodopsin adenovirus. The distribution of rhodopsin and Tctex-1 expression was determined by double-labeling for rhodopsin (red) and Tctex-1 (green). Tctex-1 was undetectable in almost all induced cells. (E) CD7-Rho39 was overexpressed in uninduced (top) or induced (bottom) T23/FLAG-RP3 monolayers via an adenovirus particle transfection method. The distribution of CD7-Rho39 in relationship to the expression of Tctex-1 was examined by double labeling of CD7 mAb (red) and Tctex-1 rabbit antiserum (green). (F) The steady-state distribution of adenovirally expressed rhodopsin in uninduced (left) or induced (right) T23/FLAG-RP3 cells was determined by domain-selective surface biotinylation followed by immunoprecipitation of rhodopsin. Immunoprecipitates were separated by SDS-PAGE and transferred to nitrocellulose. Biotinylated rhodopsin was quantitated by chemifluorescence. In three independent trials using triplicate measurements on a single cell line, rhodopsin was highly polarized to the apical surface in uninduced cells. FLAG-RP3 induction resulted in a significant loss of steady-state rhodopsin polarity. Note that rhodopsin is prone to forming higher-order aggregates on SDS-PAGE; signals from multimers were also taken into consideration in quantitation. Rhodopsin expressed in tissue culture is heterogeneously N-glycosylated (Sung et al., 1991), accounting for the broadened bands. No signal was detected from cells infected with a control recombinant adenovirus (data not shown), indicating that all of the signal seen on this blot represents rhodopsin. (G) Uninduced or induced polarized T23/FLAG-RP3 cells grown on Transwell filters were infected with rhodopsin-encoding adenovirus before pulse labeling with [^{35}S]cysteine/methionine. At 1 or 2 h of chase, cells underwent domain-selective surface biotinylation. Biotinylated rhodopsin was recovered by rhodopsin immunoprecipitation followed by precipitation with streptavidin-agarose. Samples were then digested with N-glycosidase F to reduce its aggregation on SDS-PAGE. Biotinylated, radiolabeled rhodopsin was separated by SDS-PAGE and quantitated by phosphorimaging. The percentage of total surface rhodopsin present on the apical surface at each chase timepoint is plotted. Asterisk, $P < 0.05$ between uninduced and induced cells by two-sample t test. Bar, 10 μm.

To quantify the effect on rhodopsin's polarized distribution due to Tctex-1 downregulation, T23/FLAG-RP3 stable lines were allowed to polarize under inducing or noninducing conditions and were then infected with rhodopsin adenovirus. Domain-selective surface biotinylation was then used to measure the distribution of rhodopsin on the apical and basolateral surfaces. In uninduced cells, rhodopsin was highly polarized to the apical surface (77.0 ± 3.5% apical). In contrast, induction of FLAG-RP3 resulted in a significant loss of steady-state rhodopsin polarity (54.5 ± 1.6% apical, $P < 0.001$; Fig. 6 F). Similar results were obtained in two other independent T23/FLAG-RP3 cell lines (data not shown).

In addition, we determined whether the loss of Tctex-1 disrupted rhodopsin polarity in MDCK cells by directly affecting TGN-surface vectorial transport. To this end, induced and uninduced T23/FLAG-RP3 polarized monolayers cells were infected with rhodopsin adenovirus and pulse-labeled with [^{35}S]cysteine/methionine. Cells were chased for 1 or 2 h followed by domain-selective surface biotinylation. As in our earlier report (Chuang and Sung, 1998), in uninduced cells rhodopsin was delivered directly from the TGN to the apical surface; rhodopsin was predominantly apical at both the 1 and 2 h chase timepoints (Fig. 6 G, solid bars). However, induction of FLAG-RP3 resulted in the nonpolar delivery of newly synthesized rhodopsin to the cell surface beginning at the first 1 h chase timepoint (Fig. 6 G, grey bars, $P < 0.05$ by two sample *t* test). These results suggest that Tctex-1 is contributed to the vectorial transport of rhodopsin from the TGN to the apical plasma membrane in MDCK cells.

We have shown previously that the cytoplasmic tail of rhodopsin encodes an autonomous apical sorting signal in polarized MDCK cells: addition of the COOH-terminal 39 residues of rhodopsin redirected the basolateral membrane protein CD7 to the apical membrane (Chuang and Sung, 1998). The predominantly apical localization of CD7-Rho39 fusion protein was changed to a nonpolar distribution upon Tctex-1 suppression (Fig. 6 E), whereas the basolateral localization of CD7 itself was not affected by the loss of Tctex-1 (data not shown). This result indicates that rhodopsin's COOH terminus is sufficient for Tctex-1–mediated rhodopsin apical localization in MDCK cells.

Dependence of a Subset of Endogenous MDCK Surface Proteins on Tctex-1 for Apical Transport

To verify the requirement for Tctex-1 in the apical transport of proteins intrinsic to MDCK cells, we looked for endogenous MDCK proteins whose transport to the apical surface was reduced or abolished by the induction of FLAG-RP3 expression. Polarized induced or uninduced T23/FLAG-RP3 monolayers were labeled with [^{35}S]cysteine/methionine. After a short chase period, apical surface proteins were selectively biotinylated, recovered by streptavidin-agarose precipitation, and then separated by two-dimensional gel electrophoresis. As an example, shown in Fig. 7 A, the levels of a couple of endogenous proteins (arrow) were significantly reduced at the apical surface after the induction of FLAG-RP3 expression. This result supports the notion that Tctex-1 or Tctex-1–mediated dynein activity is involved in the apical transport of a subset of endogenous MDCK membrane proteins.

Selectivity of Tctex-1-Dependent Apical Transport in MDCK Cells

We found that the distribution of the endogenous apical protein gp135 was not affected by FLAG-RP3 expression (Fig. 7 B). Similarly, influenza virus HA, which is thought to use glycolipid-cholesterol–enriched microdomains, or "rafts," for its apical transport (Simons and Ikonen, 1997), remained completely apical in RP3-expressing cells (Fig. 7 D). Finally, the endogenous basolateral proteins Na, K-ATPase (Fig. 7 C) and E-cadherin (data not shown), as well as the exogenous basolateral marker LDL receptor (Fig. 7 E), maintained their polarized basolateral distributions in MDCK cells overexpressing FLAG-RP3, suggesting that Tctex-1 suppression did not grossly disrupt basolateral protein polarity.

Discussion

Our results suggest that Tctex-1 and RP3 compete with one another for binding to a common partner within the cytoplasmic dynein complex, namely IC. Furthermore, the replacement of Tctex-1 by RP3 in the cytoplasmic dynein complex changes the apical polarity of rhodopsin in MDCK cells. These results have two important implications. First, they provide the first demonstration in living cells that cytoplasmic dynein cargo specificity, and therefore function, can be altered by subunit composition. Second, they provide the first direct evidence in living cells that cytoplasmic dynein is functionally involved in the transport of an apical membrane protein in polarized epithelia.

Cytoplasmic Dynein Function Is Regulated by Subunit Composition

Microtubules have been likened to highways for the rapid and vectorial transport of cargoes within the cell. However, a crucial problem for the cell is how to control which cargoes are allowed onto these highways at any given time. The two major classes of microtubule motors, kinesins and dyneins, have evidently developed two very different strategies to solve this problem. The kinesins are a very large superfamily of proteins (Hirokawa, 1998). It appears that each kinesin is specialized for a small or even unique subset of kinesin-mediated functions and cargoes. On the other hand, the number of genes encoding cytoplasmic dynein subunits is comparatively low. Therefore, other mechanisms must exist to regulate cytoplasmic dynein activity and cargo specificity.

One potential mechanism of dynein regulation is protein phosphorylation (Dillman and Pfister, 1994; Lin et al., 1994; Huang et al., 1999). It has been demonstrated recently that dynein–dynactin phosphorylation and dephosphorylation alters the organization of pigment granules in *Xenopus* melanophores (Reese and Haimo, 2000).

Subunit heterogeneity has also been proposed as a mechanism to regulate dynein function. Isoforms of virtually all of the known cytoplasmic dynein subunits have been identified. For example, as many as three or four cy-

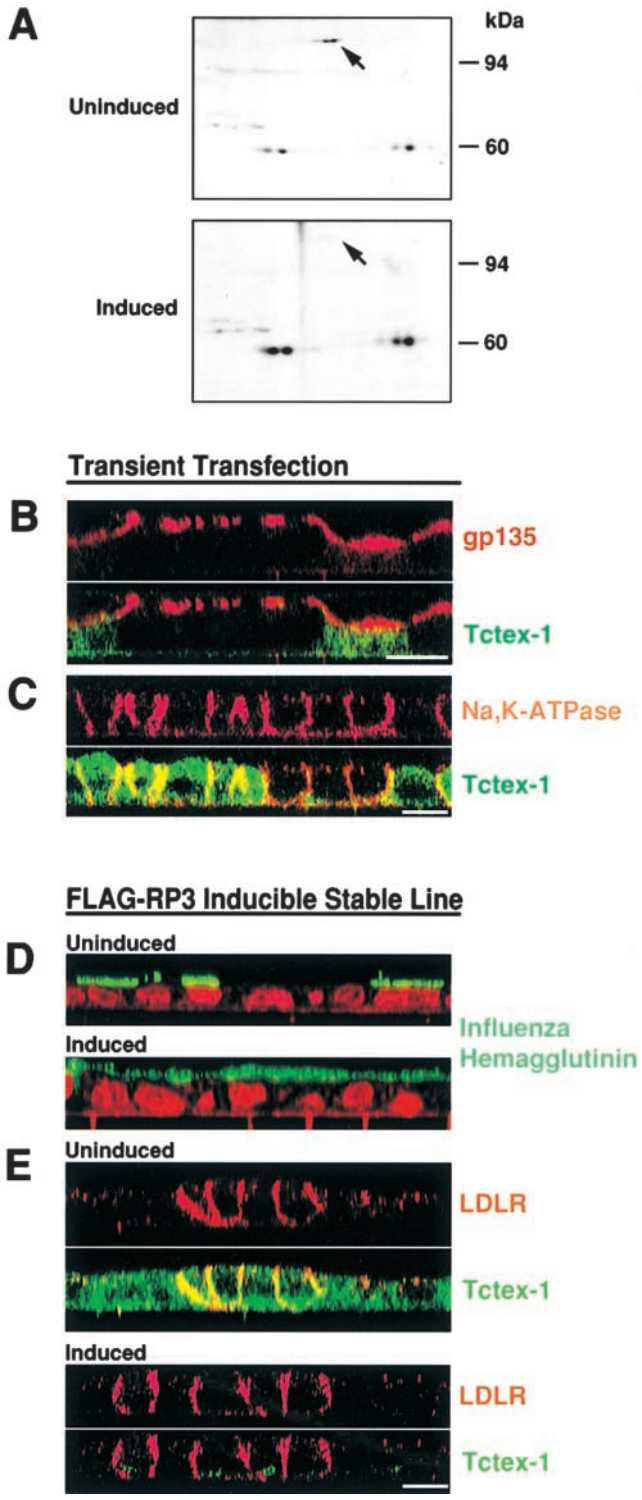

Figure 7. A subset of MDCK surface proteins requires Tctex-1 for apical transport. (A) Polarized T23/FLAG-RP3 monolayers induced to express FLAG-RP3 (bottom) or left uninduced (top) were selectively biotinylated on the apical surface after metabolic labeling with [^{35}S]cysteine/methionine. After cell lysis, biotinylated apical proteins were recovered by streptavidin precipitation and were detected by two-dimensional gel electrophoresis and autoradiography. The arrow in the top panel points to a set of proteins present on the apical plasma membrane in uninduced cells that is virtually undetectable on the apical surface after induction of FLAG-RP3 expression (bottom). The acidic end of the first dimension is to the left. (B and C) MDCK cells were transiently transfected with FLAG-RP3 and then allowed to form polarized monolayers. Cells were fixed and double-labeled with Tctex-1 antibody (green) and gp135 mAb (B, red) or Na,K-ATPase mAb (C, red). FLAG-RP3 transfected cells are identifiable by their loss of endogenous Tctex-1 expression. (D) T23/FLAG-RP3 cells were left uninduced (top) or were induced to express FLAG-RP3 (bottom) before infection with influenza virus. After fixation, cells were immunolabeled for HA rabbit antiserum (green) and counterstained with propidium iodide (red) to visualize nuclei. Duplicate filters were immunolabeled for Tctex-1 and FLAG-RP3 to verify suppression of Tctex-1 upon induction (data not shown). (E) Uninduced (top) or induced (bottom) T23/FLAG-RP3 monolayers were infected with adenovirus encoding LDL receptor (LDLR). 24 h later, cells were fixed and double-labeled with LDL receptor mAb (red) and Tctex-1 rabbit antibody (green). Bars, 10 μm.

toplasmic dynein HCs may exist, possibly with distinct tissue and intracellular localizations (Vaisberg et al., 1996; Criswell and Asai, 1998). Different pools of anterogradely transported dynein in axons have distinct IC isoform compositions (Dillman et al., 1996). The observation that different dynein subunit isoforms have different intracellular distributions provides indirect support for the existence of dynein complexes with distinct subunit compositions. However, it has not yet been shown that cytoplasmic dynein complexes with different subunit compositions actually possess different functional properties, such as cargo selectivity, in vivo.

The existence of two 14-kD dynein LCs, Tctex-1 and RP3, poses the possibility that they serve different dynein-mediated functions in vivo. This hypothesis has been further supported by the observation that the relative expression of Tctex-1 and RP3 varies greatly among and within different cellular populations of rat hippocampal formation. (Chuang et al., 2001).

The data presented in this article provide the first direct and functional evidence that dynein function is regulated by its subunit composition. We showed that altering the Tctex-1:RP3 ratio in MDCK cells changed the LC composition and, as a result, the cargo specificity, of cytoplasmic dynein. Given the sequence similarity between Tctex-1 and RP3, as well as their variable expression in different cell types, it is conceivable that both LCs can carry out a common set of dynein-mediated housekeeping functions in addition to some distinct and specific cargo recognition functions. Indeed, we found that ectopic expression of RP3 had no adverse effects on either the structural integrity of the cytoplasmic dynein–dynactin complexes, on mitosis, or on the organization of the Golgi apparatus, endosomes, or lysosomes. This is in contrast to previous approaches using the overexpression of dynactin subunits to disrupt dynein functions (Burkhardt et al., 1997; Quintyne et al., 1999). These techniques block a wide range of dynein-mediated functions, making it difficult to specifically study individual dynein functions in isolation. Instead, the replacement of Tctex-1 by RP3 appears to selectively disrupt the Tctex-1–specific functions of cytoplasmic dynein without disturbing its other functions. Therefore, this approach also appears to be very useful for identifying additional Tctex-1–dependent apical transport

processes, as well as other specific functions that Tctex-1 may have, aside from rhodopsin apical transport.

It has recently been reported that the centrosomal protein pericentrin interacts with dynein light IC (LIC; Purohit et al., 1999). In a manner analogous to the interaction of rhodopsin with Tctex-1 but not with RP3, pericentrin interacts with LIC1 but not with LIC2 in vitro (Tynan et al., 2000). However, it remains to be demonstrated that LIC1 is specifically required for pericentrin transport in vivo. Nonetheless, their findings, along with ours, strongly argue that isoform-specific binding of dynein subunits to cargo molecules may indeed be a general mechanism for generating diversity of dynein complex function.

Cytoplasmic Dynein Is Responsible for the Vectorial Transport of a Subset of Apical Proteins in MDCK Cells

The correct delivery of apical and basolateral plasma membrane proteins requires the presence of specific targeting signals. All basolateral targeting signals identified to date are located within cytoplasmic domains. It is believed that they generally function by directly interacting with cytosolic proteins, such as the AP-1 adaptor protein complex (Folsch et al., 1999). On the other hand, nearly all of the known apical targeting signals are noncytoplasmic, such as N-glycans and glycosylphosphatidylinositol anchorage (Ikonen and Simons, 1998). The mechanism by which these apical targeting signals are recognized is generally believed to involve physical partitioning into glycolipid-cholesterol–enriched microdomains, or "rafts" (Simons and Ikonen, 1997). Candidate components of an apical sorting machinery are beginning to be identified. However, the mechanisms of action of these components are not fully understood.

In contrast, rhodopsin's apical targeting signal is cytoplasmic. The apical transport of rhodopsin is unlikely to occur via a raft-associated pathway, since rhodopsin is highly soluble in cold Triton X-100 (Sung, C.-H., unpublished observation). This report provides direct evidence that the fidelity of rhodopsin apical transport in MDCK cells is dependent on Tctex-1–mediated dynein function. Together with our earlier observation that rhodopsin's apical targeting signal interacts directly with cytoplasmic dynein via Tctex-1, our results suggest that the vectorial translocation of a subset of apical membrane carriers is carried out by a direct interaction with cytoplasmic dynein. In addition, we have shown that there exist endogenous apical proteins in MDCK cells whose transport to the apical surface is dependent on Tctex-1; the identities of these proteins are currently being determined.

It has been shown previously that immunodepletion of dynein from cytosol in an in vitro transport assay reduced the efficiency of apical transport of influenza HA (Lafont et al., 1994). Interestingly, the transport of HA is generally thought to be mediated by raft microdomains (Simons and Ikonen, 1997). It would thus be of interest to investigate the possible interrelationship between rafts and microtubule-mediated transport.

The mechanisms that determine cell surface polarity appear to be fairly plastic, as the surface distributions of various proteins have been reported to vary in a tissue-dependent, and even stimulus-dependent manner (Zurzolo et al., 1992, 1993; van Adelsberg et al., 1994). In order for cells to be able to selectively control the surface distributions of different proteins, it is likely that multiple classes of apical and basolateral sorting signals exist, each with distinct mechanisms of recognition and transport that can be individually regulated from tissue to tissue. The sorting signal present in rhodopsin's cytoplasmic tail may represent an example of this functional diversity of apical targeting pathways in polarized epithelia.

We are indebted to Drs. S. Chen, P. Hargrave, W. Hong, K. Mostov, G.K. Ojakian, N.L. Weigel, M. Caplan, and E. Rodriguez-Boulan for providing reagents. We would also like to thank Mr. Kai Xu for assistance in generating the stable lines used in this study.

This work was supported by the National Institutes of Health (EY11307 to C.-H. Sung), Research to Prevent Blindness (Career Development Award and the Dolly Green Scholar Award to C.-H. Sung), the Foundation Fighting Blindness (C.-H. Sung and J.-Z. Chuang), and the Papanicolaou Medical Scientist Fellowship (A.W. Tai).

Submitted: 31 January 2001
Revised: 15 May 2001
Accepted: 18 May 2001

References

Adamus, G., A. Arendt, Z.S. Zam, J.H. McDowell, and P.A. Hargrave. 1988. Use of peptides to select for anti-rhodopsin antibodies with desired amino acid sequence specificities. *Pept. Res.* 1:42–47.

Allgood V., Y. Zhang, B.W. O'Malley, and N.L. Weigel. 1997. Analysis of chicken progesterone receptor function and phosphorylation using an adenovirus-mediated procedure for high-efficiency DNA transfer. *Biochemistry.* 36:224–232.

Bacallao, R., C. Antony, C. Dotti, E. Karsenti, E.H.K. Stelzer, and K. Simons. 1989. The subcellular organization of Madin-Darby canine kidney cells during the formation of a polarized epithelium. *J. Cell Biol.* 109:2817–2832.

Barth, A.I.M., A.L. Pollack, Y. Altschuler, K.E. Mostov, and W.J. Nelson. 1997. NH_2-terminal deletion of β-catenin results in stable colocalization of mutant β-catenin with adenomatous polyposis coli protein and altered MDCK cell adhesion. *J. Cell Biol.* 136:693–706.

Breitfeld, P.P., W.C. McKinnon, and K.E. Mostov. 1990. Effect of nocodazole on vesicular traffic to the apical and basolateral surfaces of polarized MDCK cells. *J. Cell Biol.* 111:2365–2373.

Burkhardt, J.K., C.J. Echeverri, T. Nilsson, and R.B. Vallee. 1997. Overexpression of the dynamitin (p50) subunit of the dynactin complex disrupts dynein-dependent maintenance of membrane organelle distribution. *J. Cell Biol.* 139:469–484.

Campbell, K.S., S. Cooper, M. Dessing, S. Yates, and A. Buder. 1998. Interaction of $p59^{fyn}$ kinase with the dynein light chain, Tctex-1, and colocalization during cytokinesis. *J. Immunol.* 161:1728–1737.

Chuang, J.-Z., and C.-H. Sung. 1998. The cytoplasmic tail of rhodopsin acts as a novel apical sorting signal in polarized MDCK cells. *J. Cell Biol.* 142:1245–1256.

Chuang, J.-Z., T.A. Milner, and C.-H. Sung. 2001. Subunit heterogeneity of cytoplasmic dynein: differential expression of 14-kDa dynein light chains in rat hippocampus. *J. Neurosci.* In press.

Corthésy-Theulaz, I., A. Pauloin, and S.R. Pfeffer. 1992. Cytoplasmic dynein participates in the centrosomal localization of the Golgi complex. *J. Cell Biol.* 118:1333–1345.

Criswell, P.S., and D.J. Asai. 1998. Evidence for four cytoplasmic dynein heavy chain isoforms in rat testis. *Mol. Biol. Cell.* 9:237–247.

Dillman, J.F., III, and K.K. Pfister. 1994. Differential phosphorylation in vivo of cytoplasmic dynein associated with anterogradely moving organelles. *J. Cell Biol.* 127:1671–1681.

Dillman, J.F., III, L.P. Dabney, S. Karki, B.M. Paschal, E.L.F. Holzbaur, and K.K. Pfister. 1996. Functional analysis of dynactin and cytoplasmic dynein in slow axonal transport. *J. Neurosci.* 16:6742–6752.

Folsch, H., H. Ohno, J.S. Bonifacino, and I. Mellman. 1999. A novel clathrin adaptor complex mediates basolateral targeting in polarized epithelial cells. *Cell.* 99:189–198.

Graham, F.L., and A.J. van der Eb. 1973. A new technique for the assay of infectivity of human adenovirus 5 DNA. *Virology.* 52:456–467.

Harada, A., Y. Takei, Y. Kanei, Y. Tanaka, S. Nonaka, and N. Hirokawa. 1998. Golgi vesiculation and lysosome dispersion in cells lacking cytoplasmic dynein. *J. Cell Biol.* 141:51–59.

Henkel, J.R., G.A. Gibson, P.A. Poland, M.A. Ellis, R.P. Hughey, and O.A. Weisz. 2000. Influenza M2 proton channel activity selectively inhibits trans-Golgi network release of apical membrane and secreted proteins in polarized Madin-Darby canine kidney cells. *J. Cell Biol.* 148:495–504.

Hirokawa, N. 1998. Kinesin and dynein superfamily proteins and the mechanism of organelle transport. *Science*. 279:519–526.

Huang, C.-Y.F., C.-P.B. Chang, C.-L. Huang, and J.E. Ferrell, Jr. 1999. M phase phosphorylation of cytoplasmic dynein intermediate chain and $p150^{Glued}$. *J. Biol. Chem.* 274:14262–14269.

Ikonen, E., and K. Simons. 1998. Protein and lipid sorting from the trans-Golgi network to the plasma membrane in polarized cells. *Cell Dev. Biol.* 9:503–509.

King, S.M., J.F. Dillman III, S.E. Benashski, R.J. Lye, R.S. Patel-King, and K.K. Pfister. 1996. The mouse *t*-complex-encoded protein Tctex-1 is a light chain of brain cytoplasmic dynein. *J. Biol. Chem.* 271:32281–32287.

King, S.M., E. Barbarese, J.F. Dillman, S.E. Benashski, K.T. Do, R.S. Patel-King, and K.K. Pfister. 1998. Cytoplasmic dynein contains a family of differentially expressed light chains. *Biochemistry*. 37:15033–15041.

Lafont, F., J.K. Burkhardt, K. Simons. 1994. Involvement of microtubule motors in basolateral and apical transport in kidney cells. *Nature.* 372:801–803.

Li, T., W.K. Snyder, J.E. Olsson, and T.P. Dryja. 1996. Transgenic mice carrying the dominant rhodopsin mutation P347S: evidence for defective vectorial transport of rhodopsin to the outer segments. *Proc. Natl. Acad. Sci. USA*. 93: 14176–14181.

Lin, S.X., K.L. Ferro, and C.A. Collins. 1994. Cytoplasmic dynein undergoes intracellular redistribution concomitant with phosphorylation of the heavy chain in response to serum starvation and okadaic acid. *J. Cell Biol.* 127: 1009–1019.

Martin, M., S.J. Iyadurai, A. Gassman, J.G. Gindhart, Jr., T.S. Hays, and W.M. Saxton. 1999. Cytoplasmic dynein, the dynactin complex, and kinesin are interdependent and essential for fast axonal transport. *Mol. Biol. Cell*. 10: 3717–3728.

Mok, Y.-K., K.W.-H. Lo, and M. Zhang. 2001. Structure of Tctex-1 and its interaction with cytoplasmic dynein intermediate chain. *J. Biol. Chem.* 276: 14067–14074.

O'Farrell, P.H. 1975. High resolution two-dimensional electrophoresis of proteins. *J. Biol. Chem.* 250:4007–4021.

Ojakian, G.K., and R. Schwimmer. 1988. The polarized distribution of an apical cell surface glycoprotein is maintained by interactions with the cytoskeleton of Madin-Darby canine kidney cells. *J. Cell Biol.* 107:2377–2387.

Parczyk, K., W. Haase, and C. Kondor-Koch. 1989. Microtubules are involved in the secretion of proteins at the apical cell surface of the polarized epithelial cell, Madin-Darby canine kidney. *J. Biol. Chem.* 264:16837–16846.

Paschal, B.M., H.S. Shpetner, and R.B. Vallee. 1987. MAP 1C is a microtubule-activated ATPase which translocates microtubules in vitro and has dynein-like properties. *J. Cell Biol.* 105:1273–1282.

Paschal, B.M., H.S. Shpetner, and R.B. Vallee. 1991. Purification of brain cytoplasmic dynein and characterization of its *in vitro* properties. *Methods Enzymol*. 196:181–191.

Pfister, K.K., M.W. Salata, J.F. Dillman III, K.T. Vaughan, R.B. Vallee, E. Torre, and R.J. Lye. 1996. Differential expression and phosphorylation of the 74-kDa intermediate chains of cytoplasmic dynein in cultured neurons and glia. *J. Biol. Chem.* 271:1687–1694.

Purohit, A., S.H. Tynan, R. Vallee, and S.J. Doxsey. 1999. Direct interaction of pericentrin with cytoplasmic dynein light intermediate chain contributes to mitotic spindle organization. *J. Cell Biol.* 147:481–491.

Puthalakath, H., D.C.S. Huang, L.A. O'Reilly, S.M. King, and A. Strasser. 1999. The proapoptotic activity of the Bcl-2 family member Bim is regulated by interaction with the dynein motor complex. *Mol. Cell*. 3:287–296.

Quintyne, N.J., S.R. Gill, D.M. Eckley, C.L. Crego, D.A. Compton, and T.A. Schroer. 1999. Dynactin is required for microtubule anchoring at centrosomes. *J. Cell Biol.* 147:321–334.

Reese, E.L., and L.T. Haimo. 2000. Dynein, dynactin, and kinesin II's interaction with microtubules is regulated during bidirectional organelle transport. *J. Cell Biol.* 151:155–165.

Rodriguez-Boulan, E. 1983. Polarized assembly of enveloped viruses from cultured epithelial cells. *Methods Enzymol*. 98:486–501.

Schnapp, B.J., and T.S. Reese. 1989. Dynein is the motor for retrograde axonal transport of organelles. *Proc. Natl. Acad. Sci. USA*. 86:1548–1552.

Schroer, T.A., and M.P. Sheetz. 1991. Two activators of microtubule-based vesicle transport. *J. Cell Biol.* 115:1309–1318.

Simons, K., and E. Ikonen. 1997. Functional rafts in cell membranes. *Nature.* 387:569–572.

Steffen, W., S. Karki, K.T. Vaughan, R.B. Vallee, E.L.F. Holzbaur, D.G. Weiss, and S.A. Kuznetsov. 1997. The involvement of the intermediate chain of cytoplasmic dynein in binding the motor complex to membranous organelles of *Xenopus* oocytes. *Mol. Biol. Cell*. 8:2077–2088.

Steuer, E.R., L. Wordeman, T.A. Schroer, and M.P. Sheetz. 1990. Localization of cytoplasmic dynein to mitotic spindles and kinetochores. *Nature*. 345:266–268.

Subramaniam, V.N., F. Peter, R. Philp, S.H. Wong, and W. Hong. 1996. GS28, a 28-kilodalton Golgi SNARE that participates in ER-Golgi transport. *Science*. 272:1161–1163.

Sung, C.-H., B.G. Schneider, N. Agarwal, D.S. Papermaster, and J. Nathans. 1991. Functional heterogeneity of mutant rhodopsins responsible for autosomal dominant retinitis pigmentosa. *Proc. Natl. Acad. Sci. USA*. 88:8840–8844.

Sung, C.-H., C. Makino, D. Baylor, and J. Nathans. 1994. A rhodopsin gene mutation responsible for autosomal dominant retinitis pigmentosa results in a protein that is defective in localization to the photoreceptor outer segment. *J. Neurosci.* 14:5818–5833.

Tai, A.W., J.-Z. Chuang, and C.-H. Sung. 1998. Localization of Tctex-1, a cytoplasmic dynein light chain, to the Golgi apparatus and evidence for dynein complex heterogeneity. *J. Biol. Chem.* 273:19639–19649.

Tai, A.W., J.-Z. Chuang, C. Bode, U. Wolfrum, and C.-H. Sung. 1999. Rhodopsin's carboxy-terminal cytoplasmic tail acts as a membrane receptor for cytoplasmic dynein by binding to the dynein light chain Tctex-1. *Cell*. 97:877–887.

Tynan, S.H., A. Purohit, S.J. Doxsey, and R.B. Vallee. 2000. Light intermediate chain 1 defines a functional subfraction of cytoplasmic dynein which binds to pericentrin. *J. Biol. Chem.* 275:32763–32768.

Vaisberg, E.A., P.M. Grissom, and J.R. McIntosh. 1996. Mammalian cells express three distinct dynein heavy chains that are localized to different cytoplasmic organelles. *J. Cell Biol.* 133:831–842.

van Adelsberg, J., J.C. Edwards, J. Takito, B. Kiss, and Q. al-Awati. 1994. An induced extracellular matrix protein reverses the polarity of band 3 in intercalated epithelial cells. *Cell*. 76:1053–1061.

Vaughan, K.T., S.H. Tynan, N.E. Faulkner, C.J. Echeverri, and R.B. Vallee. 1999. Colocalization of cytoplasmic dynein with dynactin and CLIP-170 at microtubule distal ends. *J. Cell Sci.* 112:1437–1447.

Zurzolo, C., C. Polistina, M. Saini, R. Gentile, L. Aloj, G. Migliaccio, S. Bonatti, and L. Nitsch. 1992. Opposite polarity of virus budding and of viral envelope glycoprotein distribution in epithelial cells derived from different tissues. *J. Cell Biol.* 117:551–564.

Zurzolo, C., M.P. Lisanti, I.W. Caras, L. Nitsch, and E. Rodriguez-Boulan. 1993. Glycosylphosphatidylinositol-anchored proteins are preferentially targeted to the basolateral surface in Fischer rat thyroid epithelial cells. *J. Cell Biol.* 121:1031–1039.